AIRESEARCH MANUFACTURING COMPANY

Los Angeles, California

HYPERSONIC RESEARCH ENGINE PROJECT - PHASE II
AEROTHERMODYNAMIC INTEGRATION
MODEL DEVELOPMENT
TWELFTH INTERIM TECHNICAL DATA REPORT
DATA ITEM NO. 55-4.12
10 DECEMBER 1970 THROUGH 9 MARCH 1971
NASA CONTRACT NO. NAS1-6666

Document No. AP-71-7279

Number of pages 31

Original date 30 March 1971

Prepared by Engineering Staff

Edited by L. F. Jilly

Approved by E N Harris

Edward N. Harris
HRE Program Manager

Revision	Date	Pages Affected (Revised, Added, Eliminated)

FORM 23771 R-70 1

FOREWORD

This interim technical data report is submitted to the NASA Langley Research center by the AiResearch Manufacturing Company, Los Angeles, California. The document was prepared in accordance with the guidelines established in paragraph 5.7.3.2.2 of NASA Statement of Work L-4947-B (Revised).

Interim technical data reports are generated on a quarterly basis for major program tasks under the Hypersonic Research Engine (HRE) Project. Upon completion of a given task effort, a final technical data report will be submitted.

This document presents a detailed technical discussion of the development of the Aerothermodynamic Integration Model (AIM) engine for the period 10 December 1970 through 9 March 1971.

CONTENTS

Section		Page
1.	SUMMARY OF STATUS	1-1
2.	PROBLEM STATEMENT	2-1
3.	TOPICAL BACKGROUND	3-1
4.	OVERALL APPROACH	4-1
5.	ANALYSIS OF AIM THRUST MEASUREMENT CORRECTION DUE TO NITROGEN PURGE	5-1
	5.1 Introduction	5-1
	5.2 Calibration	5-2
	5.3 Force Analysis	5-6
	5.4 Error Analysis	5-17
6.	FUTURE ACTION	6-1
	REFERENCES	R-1

ILLUSTRATIONS

Figure		Page
3-1	Aerothermodynamic Integration Model Nomenclature	3-2
5-1	Purge System Sketch	5-1
5-2	Discharge Characteristics of Ducted Outlets	5-8
5-3	Effect of Slot Pressure Ratio on Slot Wall Pressure	5-10
5-4	Effect of Slot Pressure on Separation Distance	5-12
5-5	Effect of Cavity Pressures on Load Cell Reading (M = 5.0)	5-13
5-6	Effect of Cavity Pressures on Load Cell Reading (M = 7.0)	5-14
5-7	Graphical Solution for Engine Drag With Zero Cavity Pressure (M = 5.0)	5-15
5-8	Graphical Solution for Engine Drag With Zero Cavity Pressure (M = 7.0)	5-16
5-9	Effect of Cavity Pressure on Absolute Tare Force	5-18
5-10	Thrust Measurement Uncertainty Due to Purge System Thrust Correction	5-20

I. SUMMARY

During this reporting period the effort expended was directed toward completing the fabrication of the various components of the HRE AIM. The effort expended by the analytical and design group was mostly in support of the fabrication of the hardware, except as noted below.

(a) Further study of the purge system necessary for the cavity bounded by the outer shell assembly and the outer cowl body was made. The design previously presented did not lend itself to fabrication and to aerodynamic loads resulting from unstart of the tunnel.

(b) Preparations were begun for establishing a format for test data acquisition and reduction.

2. PROBLEM STATEMENT

The objective of the Aerothermodynamic Integration Model (AIM) is to verify the feasibility of integrating various analytical and experimental data obtained for the design of the Hypersonic Ramjet Engine, and to evaluate the overall engine performance of this design. The design of this model will be directed to evaluating aerodynamic characteristics without major concern for the structural life of the model.

3. TOPICAL BACKGROUND

The Aerothermodynamic Integration Model (AIM) is a water-cooled, ground-test model of the Hypersonic Research Engine.

The nomenclature used to describe the various aerodynamic surfaces of this engine is shown in Figure 3-1.

General design guides followed in the design of the AIM were (1) the aerodynamic contours of the AIM were those obtained from component testing wherever possible, (2) the surface temperature of the engine was dictated by the maximum metal temperature allowable for structural integrity and by requirements of preventing boiling of the water used as the coolant, and (3) in order that the engine may be tested over the range from Mach 3 to 8, the inlet spike was mechanized to permit translation.

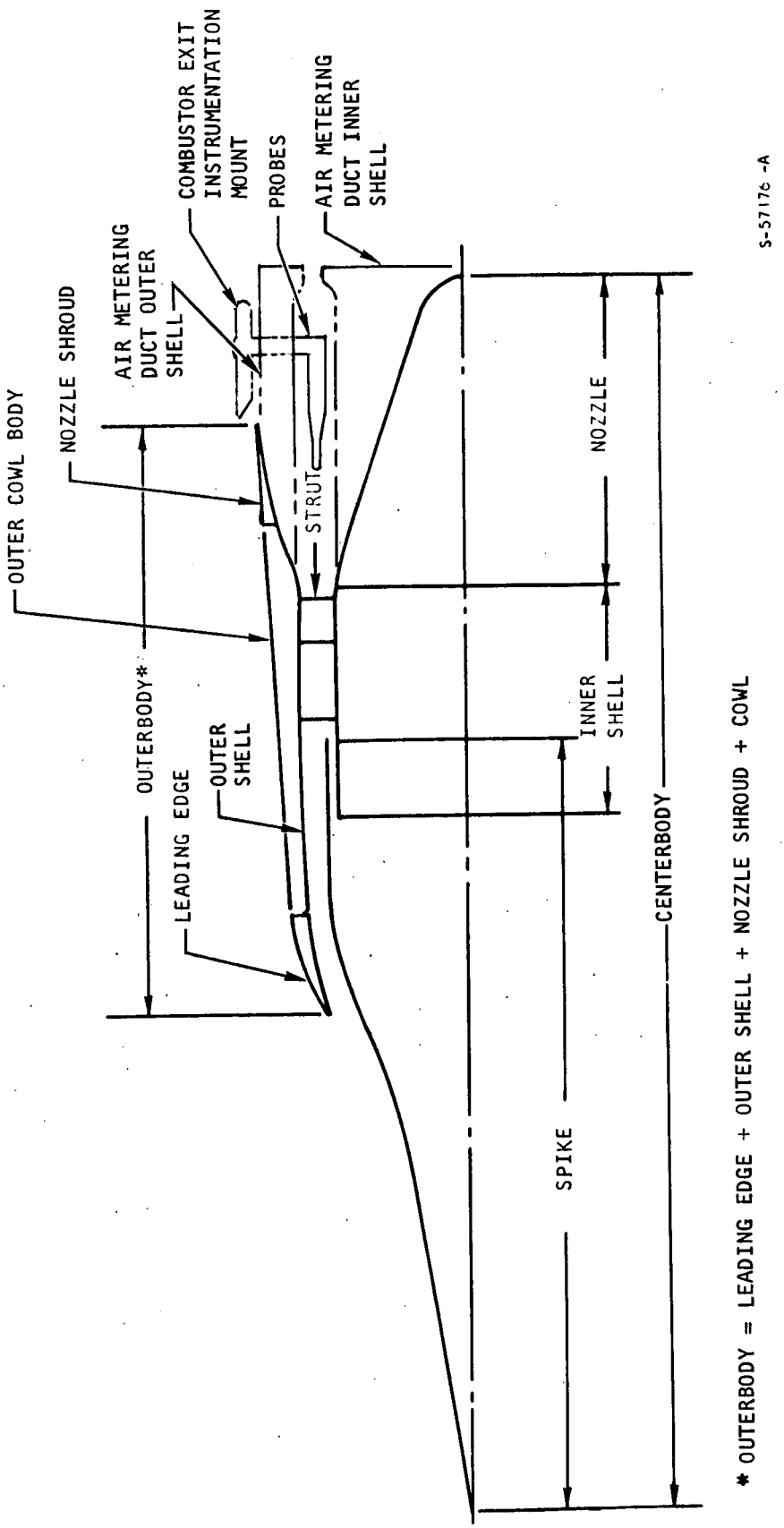

Figure 3-1. Aerothermodynamic Integration Model Nomenclature

4. OVERALL APPROACH

The basic design concepts previously submitted were used in the component layout drawing. However, due to the diverse requirements imposed upon the design to satisfy the considerations of thermal analysis, structural design, mechanical design and manufacturing techniques, tests will be conducted to determine the internal aerodynamic performance over Mach number range of 5.0 to 7.0. The effects of varying inlet air total pressure and temperature, fuel-air ratio, inlet spike position, and combustion mode will be investigated. All tests will be conducted with clean air. The measured performance will have to be corrected to account for heat removed by the water-cooling system.

Tests will be performed to

(a) evaluate the inlet-combustor interaction and stability

(b) evaluate the performance of the positive ignition system

(c) identify conditions when autoignition is feasible

(d) demonstrate combustion mode transition

(e) evaluate inlet and combustor performance

(f) determine overall engine performance

(g) determine engine operating characteristics with feasible variations in fuel equivalence ratio

(h) determine nozzle performance for the purpose of substantiating the predicted overall engine performance, including chemical kinetic effects

5. ANALYSIS OF AIM THRUST MEASUREMENT CORRECTION DUE TO NITROGEN PURGE

This section presents an analysis of forces introduced to the thrust balance during AIM testing due to nitrogen purge. A method of determining the purge system thrust calibration by direct load cell measurement is proposed, and an error analysis is presented.

5.1 INTRODUCTION

Purge nitrogen must be fed into the cavity between the AIM hot shroud and the outerbody to prevent entry of the hot tunnel flow. When the cavities are pressurized, a tare force is applied to the load cell. This force must be known so that the necessary correction can be applied to the load cell reading to determine thrust. The purge nitrogen is discharged from the cavity through slots at the leading and trailing edges of the hot shroud and through the legs. Because of static pressure variations on the AIM surfaces, the forward slot requires about three-times the pressure as the aft slot to prevent entry of the hot flow. A seal will be installed dividing the cavity into two compartments as shown in Figure 5-1.

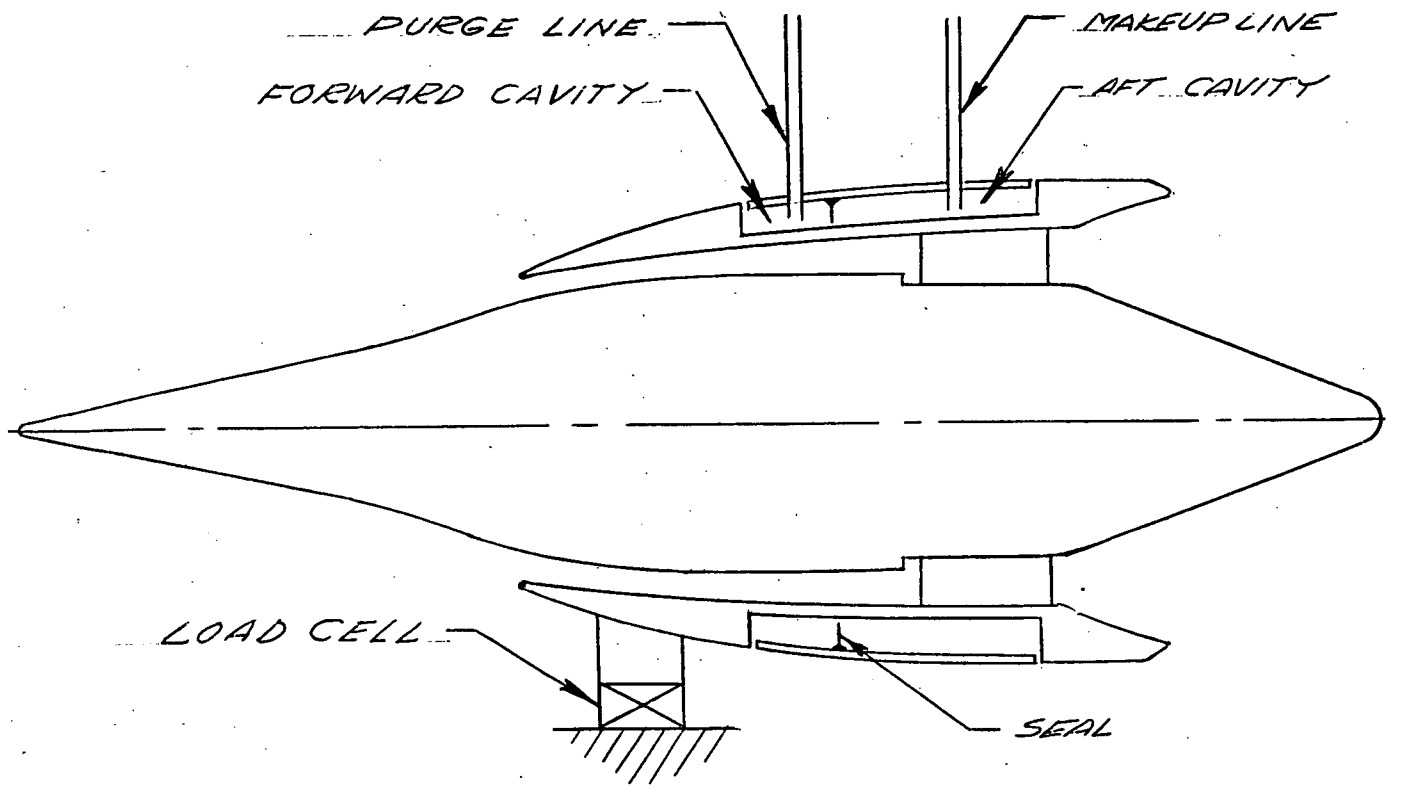

Figure 5-1. Purge System Sketch

The seal has been positioned so that the front cavity has a larger projected area in the thrust direction than the aft cavity by a factor of about three. Without the seal, the entire cavity would operate at the pressure required by the front slot, resulting in a higher tare force. A simple calculation using a factor of three on both the pressures and the projected areas described above shows that the absolute value of the tare force is reduced by a factor of two when the seal is installed. This will result in a corresponding reduction in thrust measurement uncertainty.

Referring to Figure 5-1, the nitrogen is supplied into the forward cavity by the purge line. The nitrogen flow rate is controlled by an Annin valve to set the cavity pressure at the desired value. Some of the nitrogen leaks through the seal to pressurize the aft cavity. The leakage rate is insufficient to obtain the desired aft cavity pressure. The makeup line supplies the remaining nitrogen to set the pressure. The design flow rate and pressure for the purge line is 4.5 lb/sec at 700 psia at the AIM inlet flange. The corresponding values for the makeup line are 1.5 lb/sec and 700 psia. The detail design requirements for the system are described in Reference 1.

The tare force depends on the front and rear cavity pressures and the tunnel Mach number and total pressure. Also, some effects are expected to be encountered due to the interaction of nitrogen flow and the external flow. The nitrogen jet leaving the front cavity will cause a shock wave to stand on the engine cowl and an associated increase in cowl drag. Also, the pressure on the cavity walls near the exit may be affected by interaction with the external flow. If the tunnel Mach number distribution varies with inlet flow properties, the tare may be influenced. Accurate calculation of the tare force thrust correction is difficult because of the complex nature of the problem. Integration of the tare force using pressure tap data is unattractive because of insufficient instrumentation.

The following section presents an analytical estimate of the tare forces and a method for calibrating the tare force by direct load cell measurement while the tunnel is in operation. The major problem here is that during a calibration run, the load cell measures the engine drag plus the tare force. The unknown drag must be evaluated and subtracted from the load cell reading to determine the tare.

5.2 CALIBRATION

5.2.1 Calibration Tests

It is proposed that force calibration runs first be made with the engine installed in the tunnel with no external flow. The purpose of the tests is to determine flow rates and supply pressures and provide a system checkout. The forward and aft cavity pressures will be varied to determine their effect on load cell reading. The data will serve as a cross-check on similar tests with external flow. The external flow tests will be performed at each tunnel Mach number to determine the effect of the cavity pressures including the interactions with the external flow.

The effect of tunnel total pressure on the calibration must be spot-checked. This is discussed further in Section 5.2.3. Also, the spike position must be varied to investigate a possible effect on the calibration. The spike position may affect the front slot approach Mach number, thereby affecting the cowl drag increment due to shock from the nitrogen jet. A wide range of cavity pressures must be investigated, including those approaching the no-purge flow condition. Therefore, the tests should be performed at as low a tunnel temperature as possible; this will prevent damage to the AIM in case external flow inadvertently enters the cavities. An orifice meter should be placed in each purge line to show when the purge flow is at a minimum allowable value. Pressure regulators should also be installed in the two supply lines so that one pressure can be varied while the other is held constant, otherwise the data cannot be plotted in a comprehensive manner.

5.2.2 Determination of Engine Drag

The calibration data will be plotted as shown below.

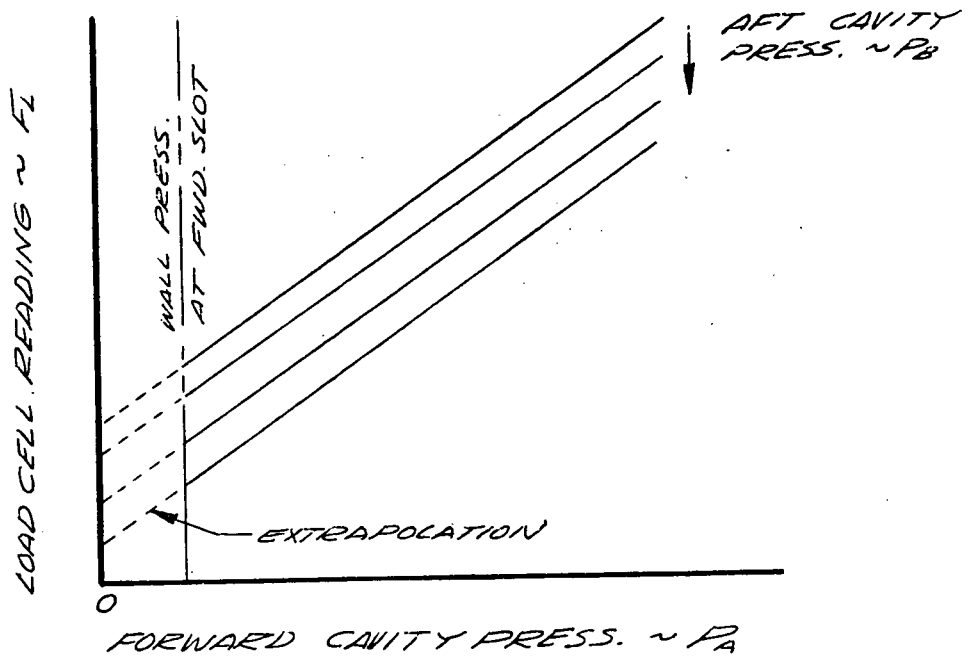

The lines of constant P_B will be extrapolated to $P_A = 0$. The $P_A = 0$ intercepts will then be cross-plotted as shown below.

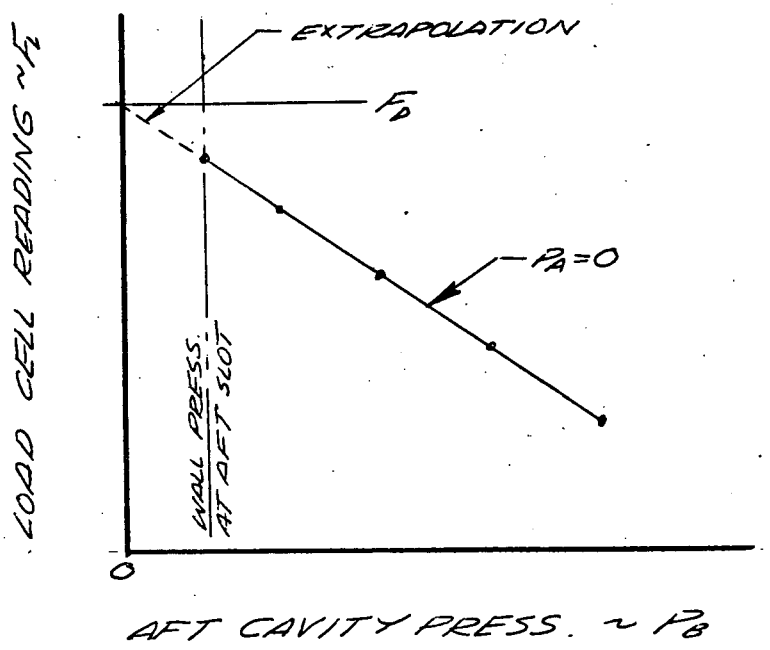

The $P_B = 0$ intercept of this plot gives the load cell reading, F_D, when both the forward and aft cavity pressures are zero. F_D is then the sum of all drag forces acting on the engine other than the forces caused by the introduction of the purge nitrogen including the effect of interactions with the external flow. F_D is defined in detail in Section 5.3.

5.2.3 Thrust Calibration Curve

F_D can be subtracted from F_L to obtain the force, F_T, exerted on the AIM due to nitrogen purge. Included in F_T is the increment in cowl drag, ΔF_S, due to the shock. It is inconvenient to include ΔF_S in F_T for the thrust correction. Therefore, ΔF_S will be evaluated using the cowl pressure taps during the calibrations and subtracted from F_T to obtain the net correction factor F_T'.

F_T' will be plotted as shown below.

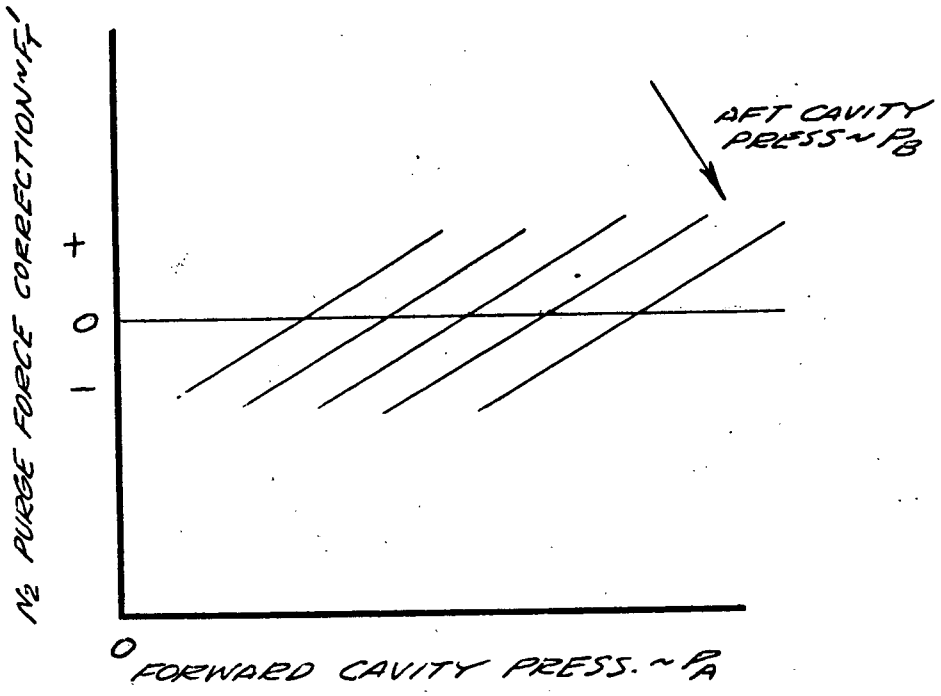

Curves of this type will be input into the data analysis computer program to correct the load cell reading. It can be shown that this curve may be put in parametric form as

$$\frac{F_T'}{P_{T0}} = f\left[\frac{P_A}{P_{T0}}, \frac{P_B}{P_{T0}}\right]$$

This will provide a convenient means of accounting for variation in the tunnel total pressure. The use of this method must be verified experimentally by spot-checking the calibration at various values of P_{T0}.

The uncertainty in the determination of the calibration by this method depends on the following variables:

The amount of scatter and accuracy of the load cell reading and pressure data taken

The amount of extrapolation required to reach the zero-pressure intercepts

The linearity of the calibration data

The final evaluation of the accuracy of this method can only be made after the data has been taken and analyzed. The accuracy is further discussed in Section 5.4.

5.3 FORCE ANALYSIS

To obtain a feel for the validity of the proposed calibration method, the calibration curves have been analytically predicted. The tunnel conditions selected for the analysis are Mach 5 at 415 psia and Mach 7.0 at 1000 psia. The analysis may prove useful for interpreting the test results. It is also possible that the data may be analytically extrapolated using the equations derived in the analysis and constants obtained from data reduction.

5.3.1 Analytical Model

The following model is used to analyze the forces exerted on the load cell due to the cavity pressures.

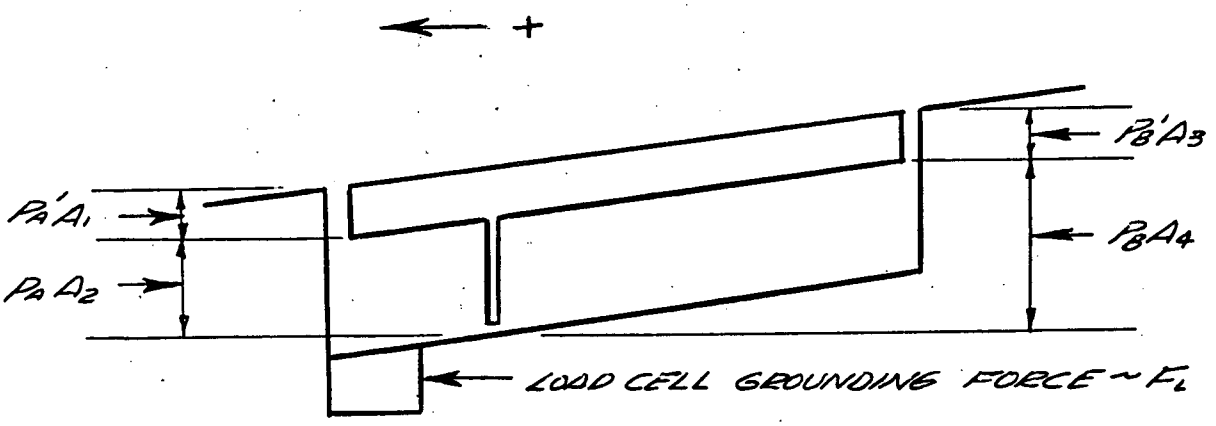

CAVITY FORCES

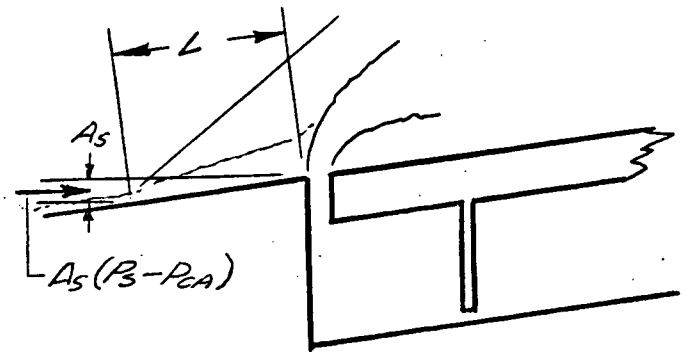

P_{CA} = Cowl pressure with no shock

P_S = Cowl pressure with shock

Force increment due to shock = $A_S(P_S-P_{CA}) = \Delta F_S$

SHOCK FORCE

The load cell grounding force, F_L, is given by a summation of forces in the thrust direction.

$$\Sigma F_X = 0$$

$$F_L = -F_D - A_S \left(P_S - P_{CA}\right) + P'_A A_1 + P_A A_2 - \left(P'_B A_3 + P_B A_4\right) \qquad (1)$$

F_D is the sum of internal and external drag forces on the engine and is composed of the following elements.

The change in stream thrust of the internal flow

Inlet additive drag

Cowl drag with no shock due to the nitrogen jet

Boattail force

F_D has an estimated value of -1450 lb at Mach 5, and -770 lb at Mach 7. These values were obtained from Reference 2, Figure 1.

The assumptions and procedures for evaluating the pressures used in Equation (1) are discussed in the following paragraphs.

5.3.2 Cavity Pressures

The pressures P_A and P_B in the cavities are assumed to act on the projected areas A_2 and A_3 at full value. The attempt was made to account for the small pressure drops as the purge flow passes the manifolds and other obstructions in the cavities.

5.3.3 Slot Flow Characteristics

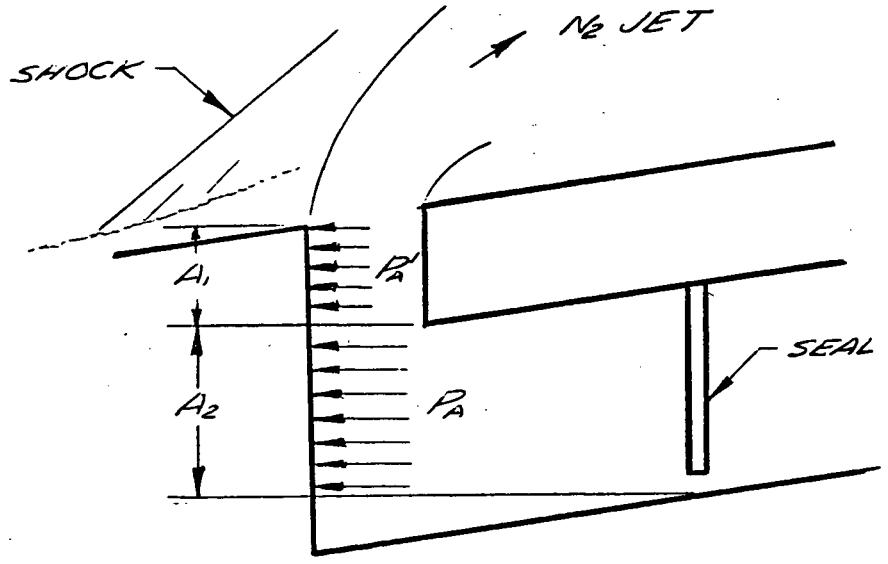

The pressures acting on the area A_1 are less than the pressures on A_2 because of the reduction in static pressure when flow is established. The aerodynamics of this process require special attention because of the interaction with the external flow.

Reference 2 presents the flow characteristics of a rectangular duct discharging into a Mach 3.85 stream. This report was used to

Predict the static pressures P'_A and P'_B on the slot walls contributing to the load cell forces

Predict the slot choking pressure ratios

Predict the pressure required to establish flow in the slots

Figure 5-2 is a curve from Reference 3 showing the sonic flow coefficient, K_S, as a function of $P_{T,0}/P_0$. This ratio is the total pressure in the slot divided by the static pressure in the undisturbed flow upstream of the slot.

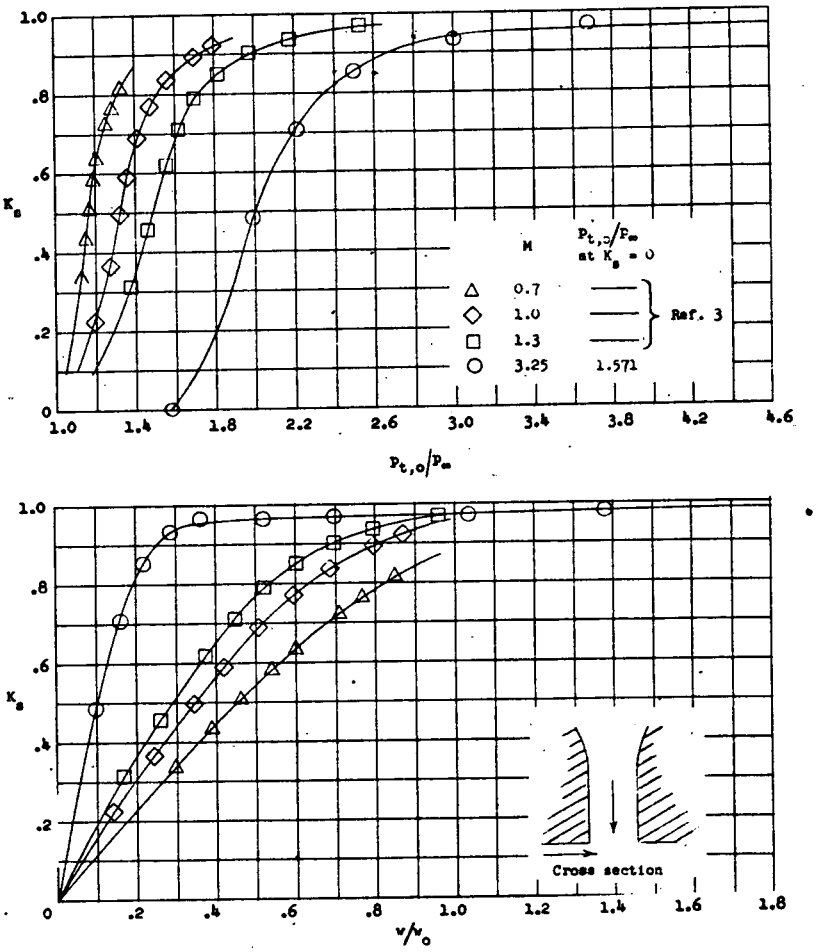

(a) Square ducted outlet 9. A = 1.0; $\beta = 90^\circ$.

Figure 5-2. Discharge Characteristics of Ducted Outlets

The sonic flow coefficient is defined as follows:

$$K_S = \frac{\text{measured slot flow}}{\text{theoretical slot flow at sonic velocity}}$$

$$= \frac{W}{\dfrac{0.532\ P_{T,0}\ A_{slot}}{\sqrt{T_{T,0}}}}$$

Figure 5-2 shows that

(a) A pressure ratio of 1.57 is required to establish flow in the slot at $M_0 = 3.25$.

(b) A pressure ratio of approximately 3.0 is required to choke the slot at $M_0 = 3.25$.

(c) The relationships in (a) and (b) above depend on slot approach Mach number.

Since the intent of this analysis is to show trends only, the Mach 3.25 data was used directly for both the front and rear slots. The actual slot approach Mach numbers probably lie between 2.5 and 3.5 for both $M_0 = 5$ and 7 which are analyzed herein.

Reference 2 presents data which shows that the slot start-flow- and choking-pressure ratios depend on aspect ratio for outlets through a thin plate. These relationships are not known for outlets with an approach duct as encountered in the AIM. It is not felt that this uncertainty will affect the trends shown in the analysis. It is conservative to assume that the start-flow- and choking-pressure ratios are high because this increases the extrapolation distance required to reach the zero-pressure intercepts.

5.3.4 Slot Wall Pressures

The pressures P'_A and P'_B were estimated using the data from Figure 5-2 as follows: To calculate the slot Mach numbers, the relationship

$$\left(\frac{A}{A^*}\right)_{SLOT} = \frac{K_{S\ MAX}}{K_S}$$

and

$$P_{SLOT} = P' = \left(\frac{P_S}{P_T}\right)_{SLOT} P_{T\ SLOT}$$

$$= f\left(\frac{A}{A^*}\right)_{SLOT} P_{T\ SLOT}$$

This relationship was used to plot the curve presented in Figure 5-3 which was used to obtain the slot wall pressures P'_A and P'_B.

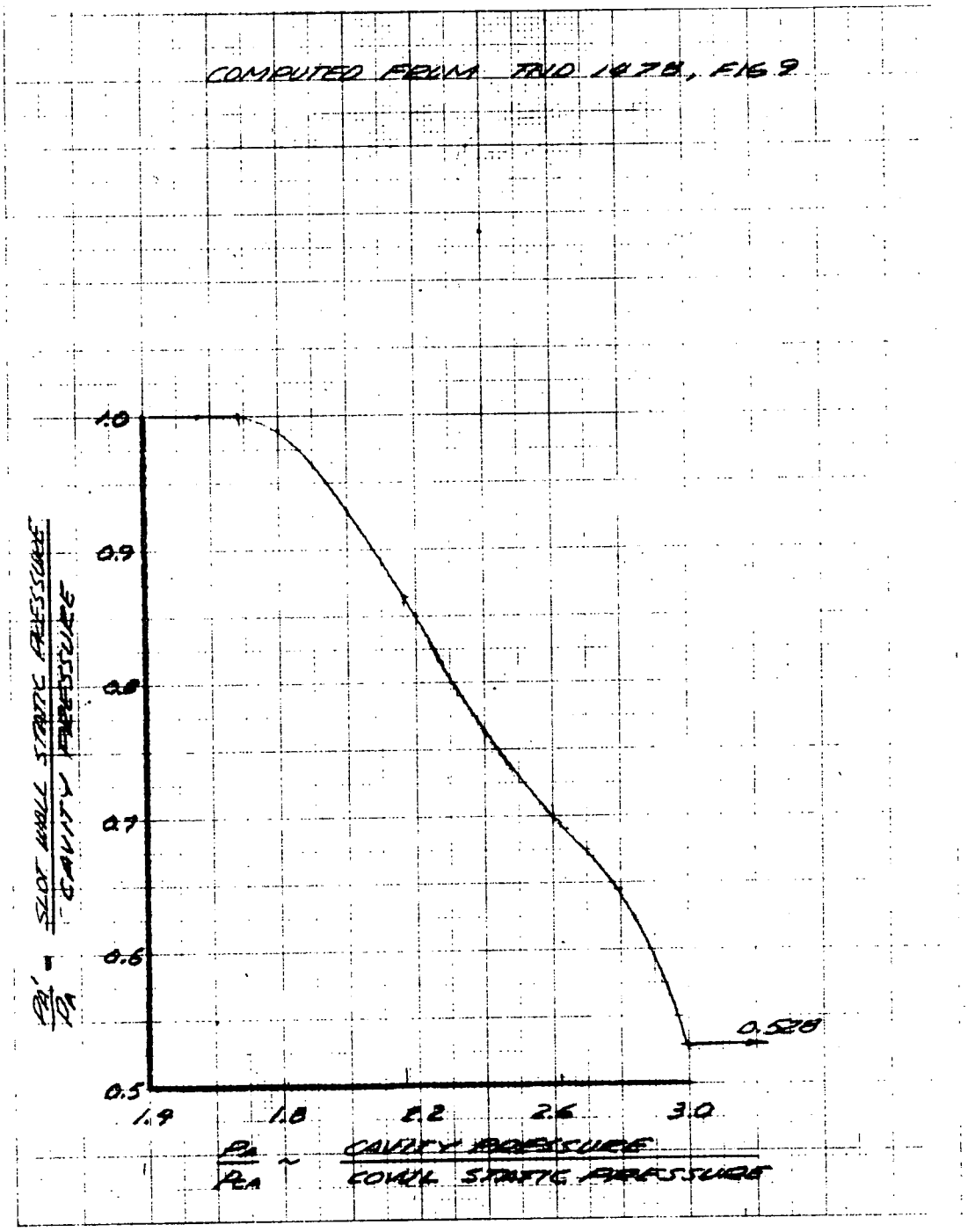

Figure 5-3. Effect of Slot Pressure Ratio on Slot Wall Pressure

5.3.5 Outer Skin Pressures

The AIM wall static pressures just upstream of the slots with no purge flow were taken from measured values from the Langley tunnel starting tests using configuration IV-shroud $4X_1$. These data were taken at Mach 5. The measured front slot pressure ratio, P_{CA}/P_0, was 7.0. The aft slot pressure ratio, P_{CB}/P_0 was 2.0. To convert these pressure ratios to Mach 7 values, $\Delta P/q_0$ was assumed to be the same for the two Mach numbers.

5.3.6 Shock Force

The force due to the impingement of the shock generated by the N_2 jet at the front slot is done as follows. The separation distance, L, was determined from an analysis presented in Reference 4, Figure 5.34. Figure 5-4, which is derived from this reference, presents L as a function of forward cavity pressure, P_A, divided by cowl static pressure, P_{CA}, in the undisturbed flow. It was assumed for this analysis that the separation distance is independent of freestream Mach number.

The static pressure acting on the affected area was assumed to be 2.5-times higher than the undisturbed pressure. Thus $P_S = 2.5\ P_{CA}$.

5.3.7 Results

Figures 5-5 and 5-6 show the computed load cell readings from Equation (1) for a range of assumed cavity pressures.

The internal plus external drag of the AIM, F_D, assumed for each Mach number is spotted on the curves. The extrapolations to $P_A = 0$ are also shown. The extrapolations were performed by extending the linear portion of the curves above the slot-choking pressure.

It can be shown that theoretically both the linear and nonlinear portions of the curves extrapolate to the same point. This provides a cross check when the calibration data is analyzed. If a discrepancy occurs, a judgment will be made based on inspection of the data. If the choked portion of the curves proves to be truly linear, the intercepts may be determined analytically using $y = mx + b$.

The FL at $P_A = 0$ values determined by the extrapolations are cross-plotted in Figures 5-7 and 5-8. These curves provide the final solution for the AIM drag, F_D, at zero cavity pressure.

The drag assumed in the analysis is spotted on the curves so that the alignment of the plotted curve with the known solution can be observed. The target area for a one-percent thrust error is spotted on the curves. Under the

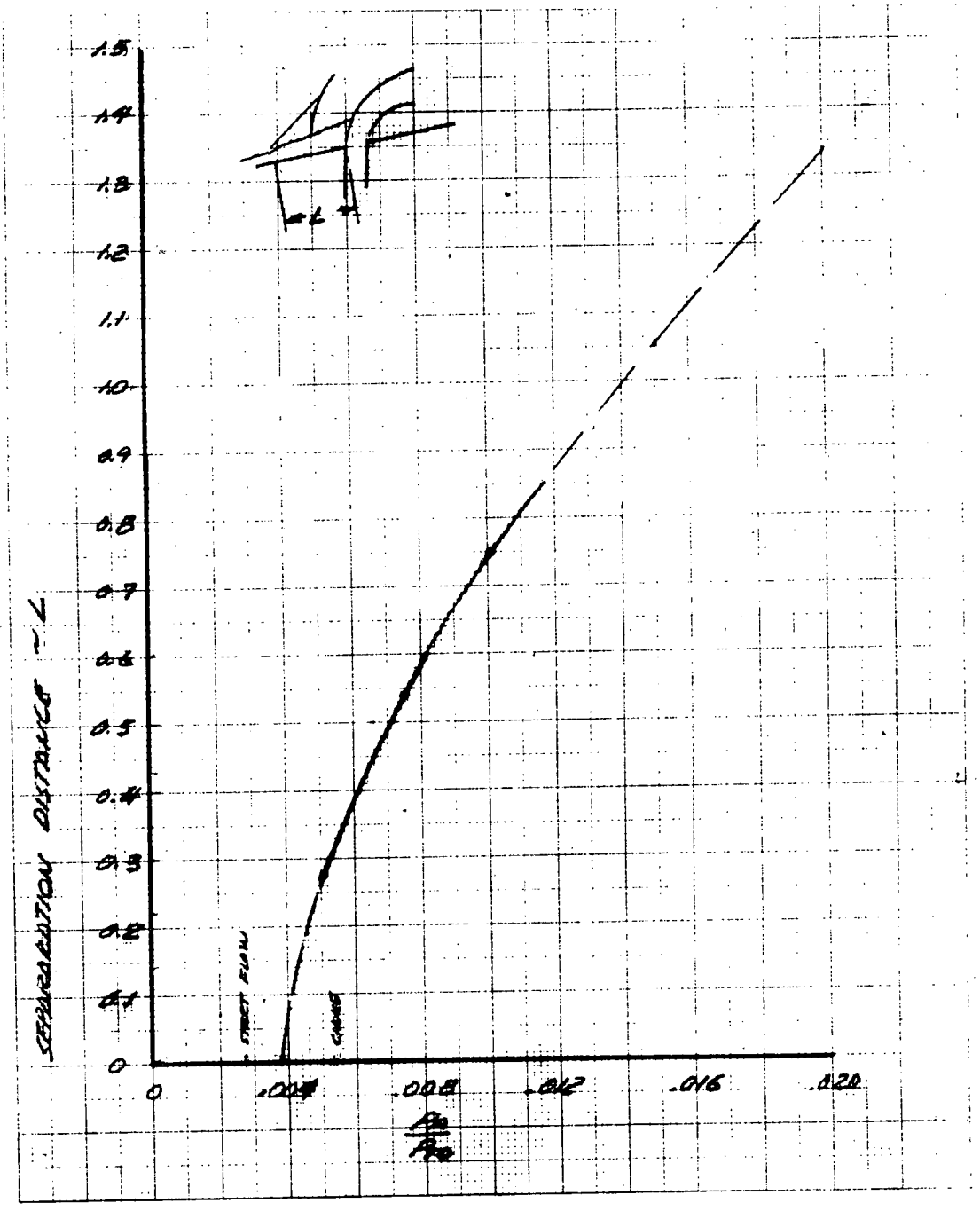

Figure 5-4. Effect of Slot Pressure on Separation Distance

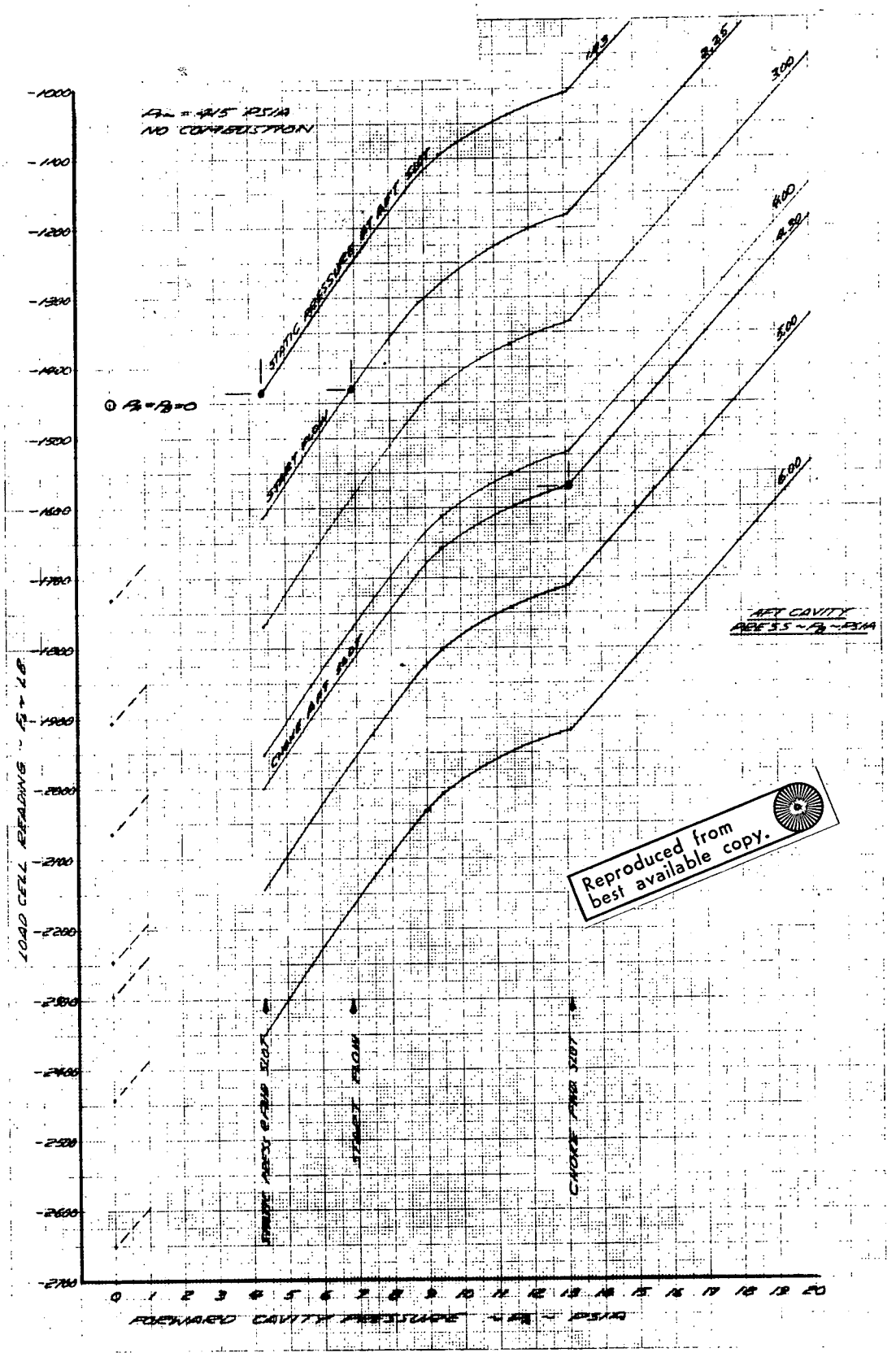

Figure 5-5. Effect of Cavity Pressures on Load Cell Reading (M = 5.0)

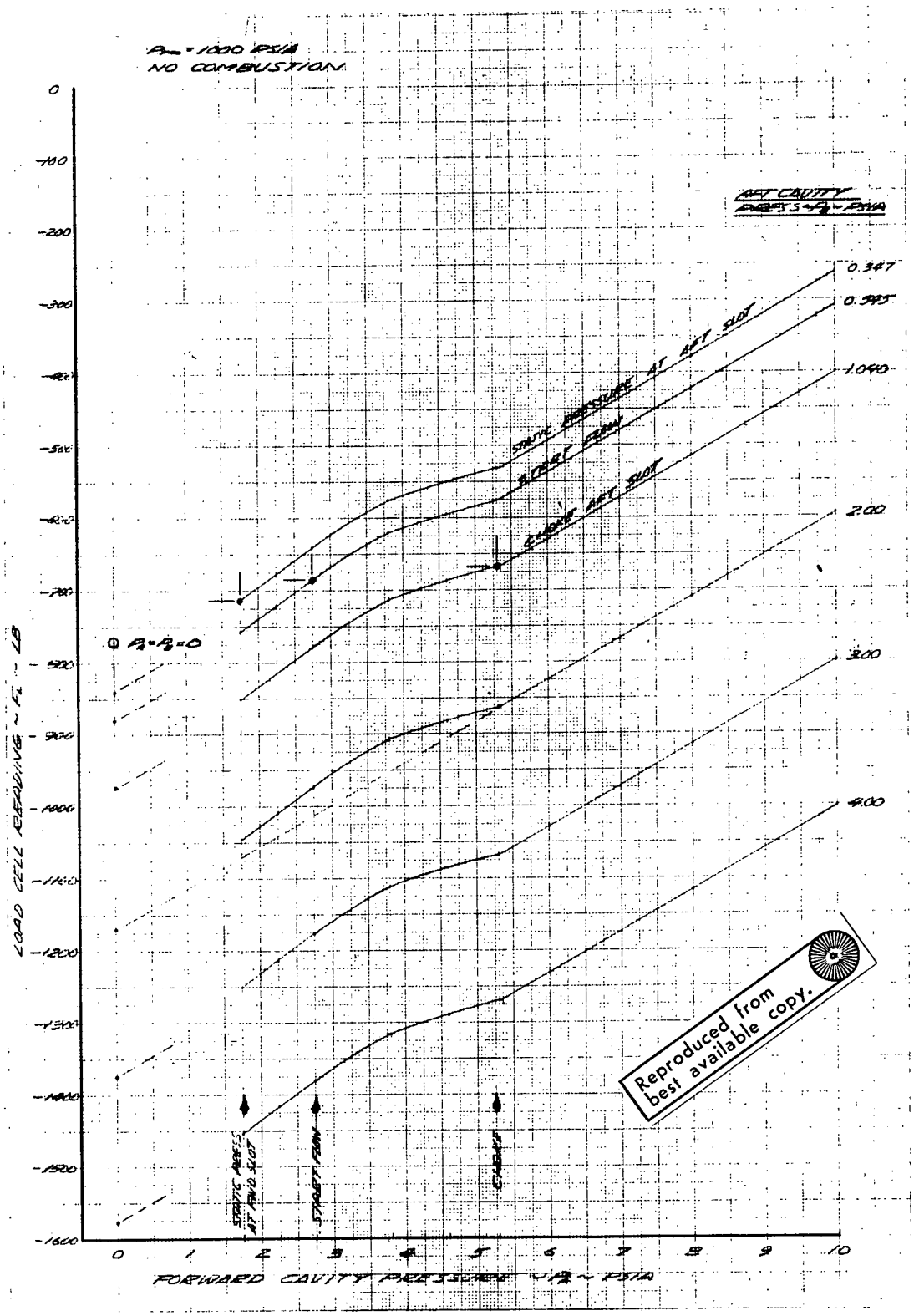

Figure 5-6. Effect of Cavity Pressures on Load Cell Reading (M = 7.0)

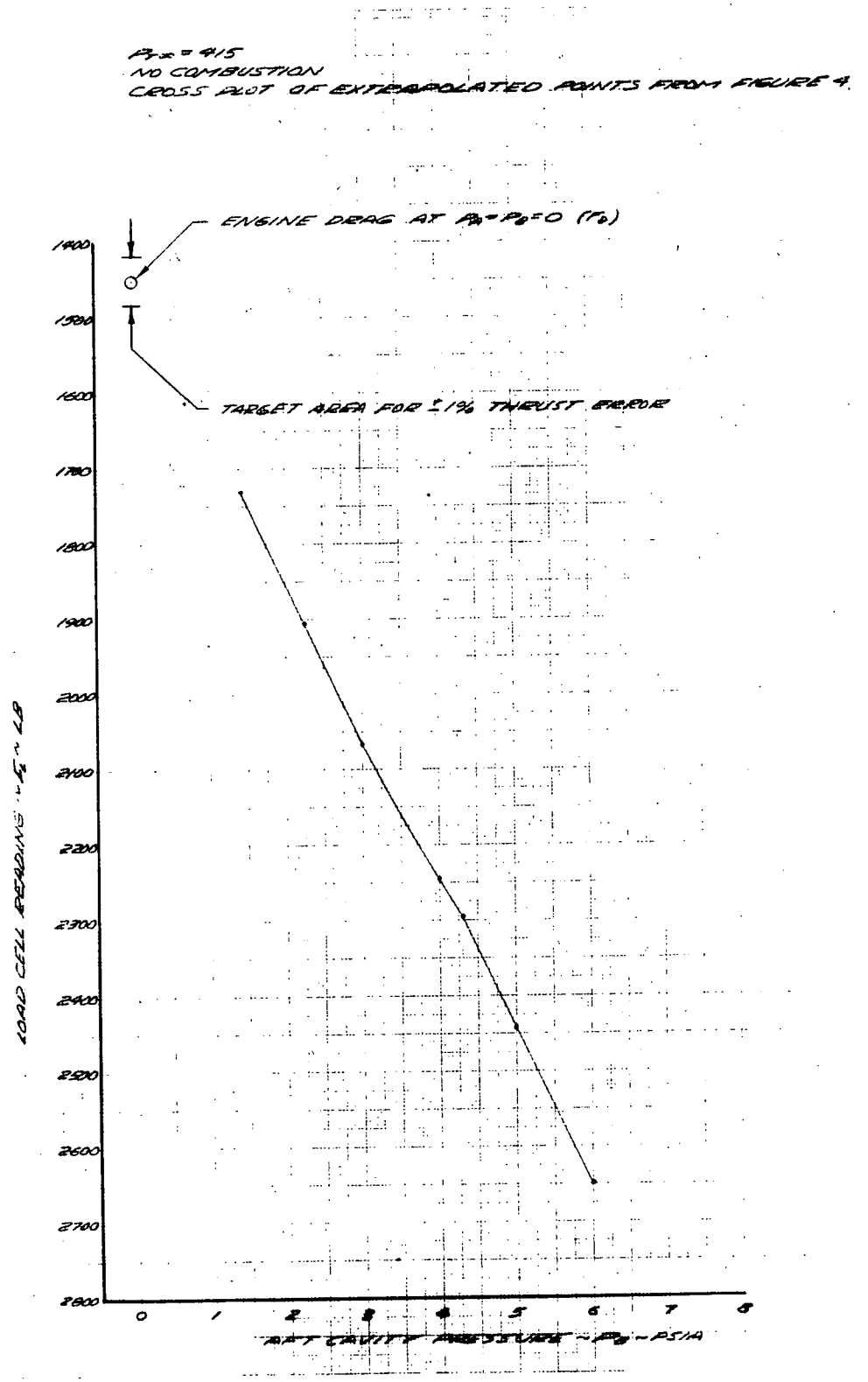

Figure 5-7. Graphical Solution for Engine Drag With Zero Cavity Pressure (M = 5.0)

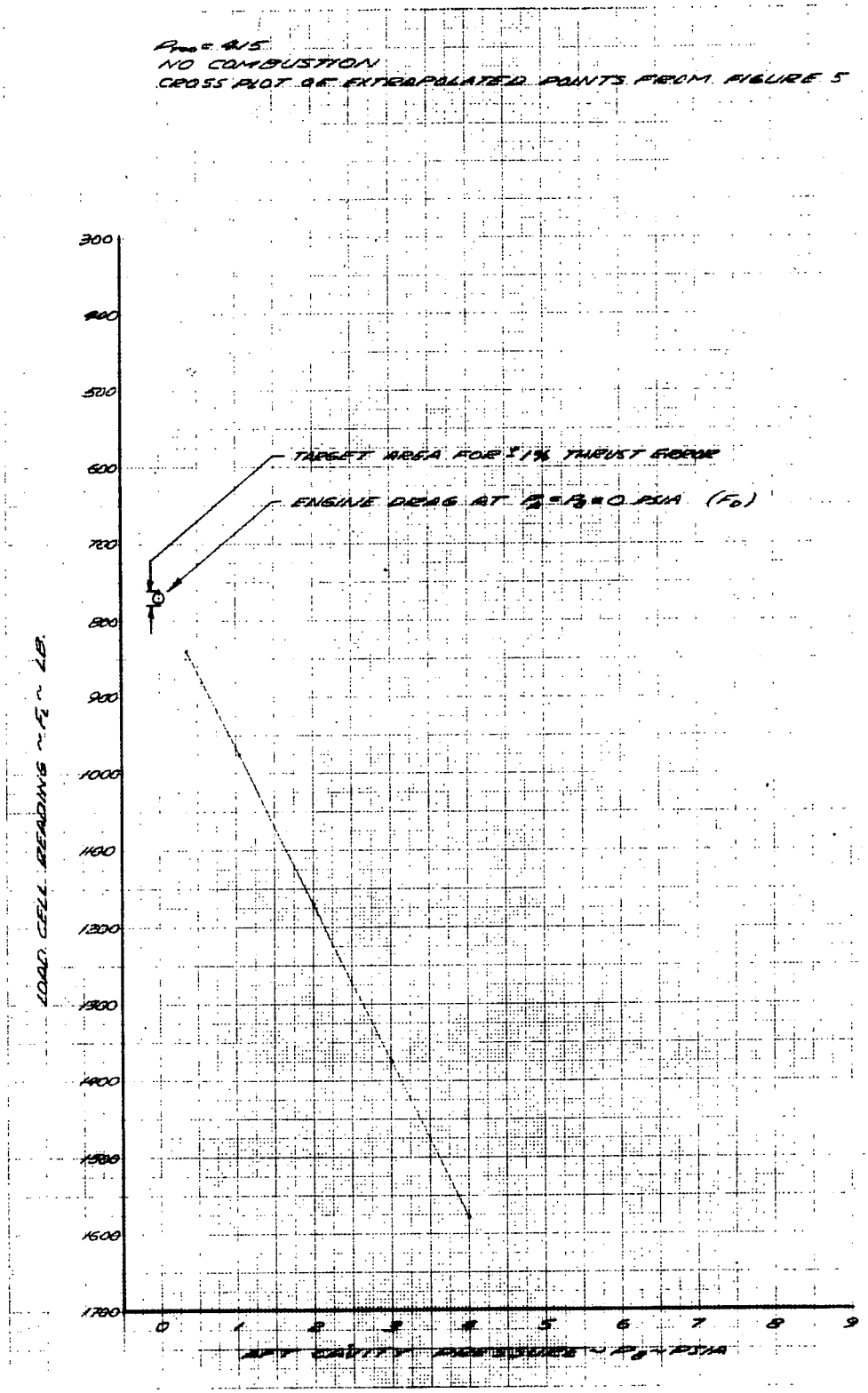

Figure 5-8. Graphical Solution for Engine Drag With Zero Cavity Pressure (M = 7.0)

ideal conditions of plotting analytical results, a reasonably accurate extrapolation appears to be feasible.

5.4 ERROR ANALYSIS

The tare force due to purge is given by the following equation:

$$F_T = A_S \left(P_S - P_{CA}\right) + P'_A A_1 + P_A A_2 - \left(P'_B A_3 + P_B A_4\right) \qquad (2)$$

It is planned to run the AIM tests with P_A and P_B set so that F_T has a net value of zero. The pressures required to do this will be determined from the calibration tests.

However, the thrust uncertainty due to the purge system is independent of the net value of F_T. The uncertainty depends on the total force exerted on the AIM by the purge system. This can be evaluated by taking the absolute value of Equation (2).

$$\left|F_T\right| = A_S \left(P_{CS} - P_{CA}\right) + P'_A A_1 + P_A A_2 + P'_B A_3 + P_B A_4 \qquad (3)$$

$\left|F_T\right|$ from Equation (3) is plotted versus P_A at a value of $F_T = 0$ in Figure 5-9. The values of P_A and P_B required to hold $F_T = 0$ can be read from Figures 5-5 and 5-6 at the intersections of the P_B lines with $F_L = F_D$.

$\left|F_T\right|$ is seen to be nearly linear with P_A. With the assumption that $\left|F_T\right|$ is linear with cavity pressures, the effects of pressure and force measurement undertainties were evaluated with the following ground rules:

A ±1-percent uncertainty in P_A and P_B pressure measurements during performance tests. This gives a ±1-percent uncertainty in $\left|F_T\right|$.

A ±1-percent uncertainty in P_A and P_B during calibration tests. This gives an additional ±1-percent unertainty in $\left|F_T\right|$.

A ±1-percent uncertainty in load cell reading during calibration tests. Since the error analysis is done at a net tare force of 0, the load cell reading will be equal to the AIM drag at zero cavity pressure, F_D. F'_D has a predicted value of 770 lb at Mach 7 and 1450 lb at Mach 5.

The AIM thrust was taken from Reference 2 at the minimum values for the thrust loads presented.

No attempt was made to evaluate the error due to the extrapolated

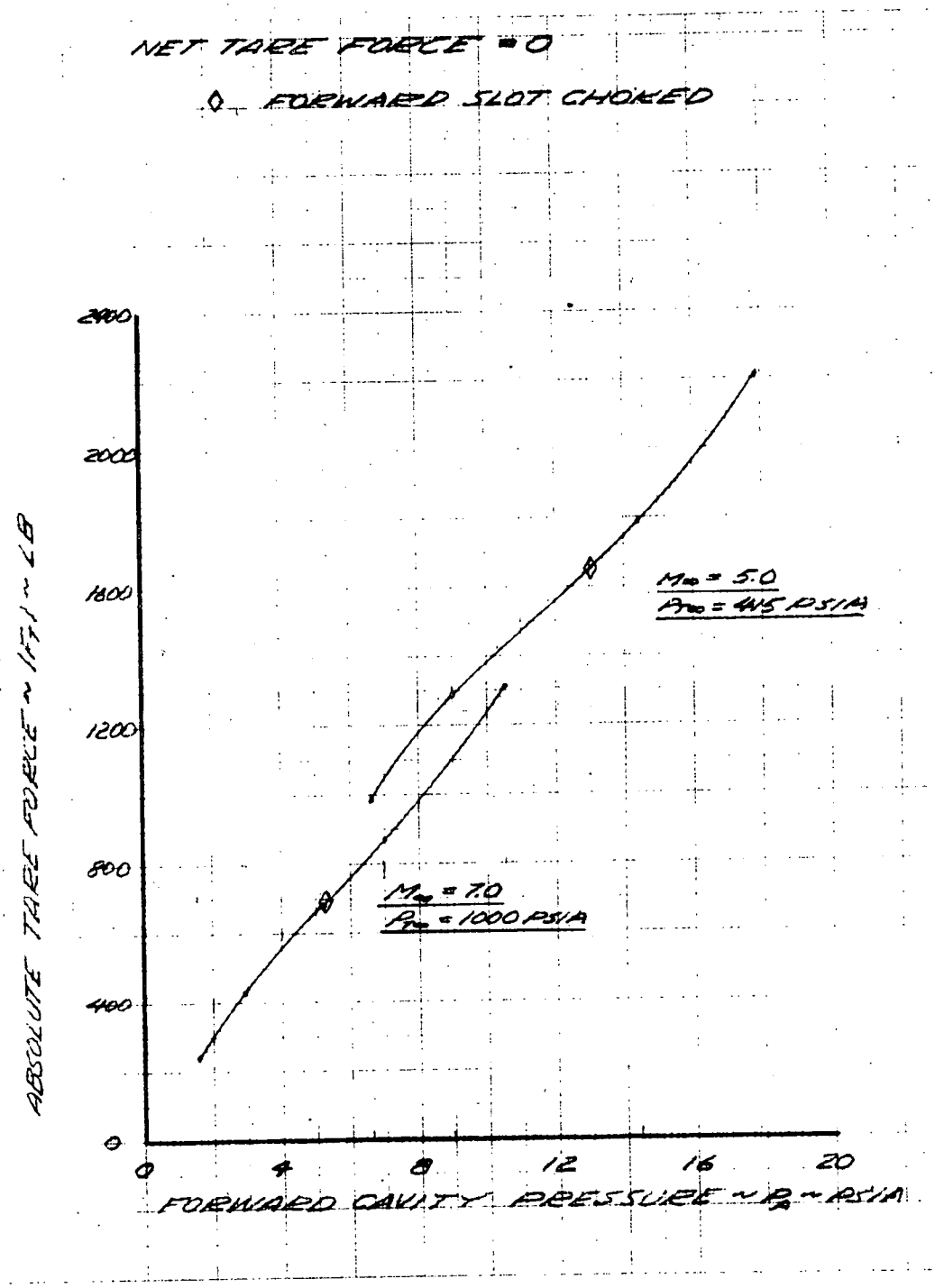

Figure 5-9. Effect of Cavity Pressure on Absolute Tare Force

solution for F_D. The uncertainty due to the extrapolation will be evaluated when the calibration data is reduced and the various methods of extrapolation are cross-checked.

Figure 5-10 presents the thrust uncertainty with the above ground rules and assumptions. The error is seen to increase P_A. This implies that the cavity pressures should be set as low as possible to reduce the error. The point can be made that the pressure should be sufficiently high to choke the slots. This could minimize the interactions between the cavity pressures and the external flow and thereby reduce the error. The values of P_A and P_B used for the AIM performance tests will be selected when the calibration test data have been analyzed.

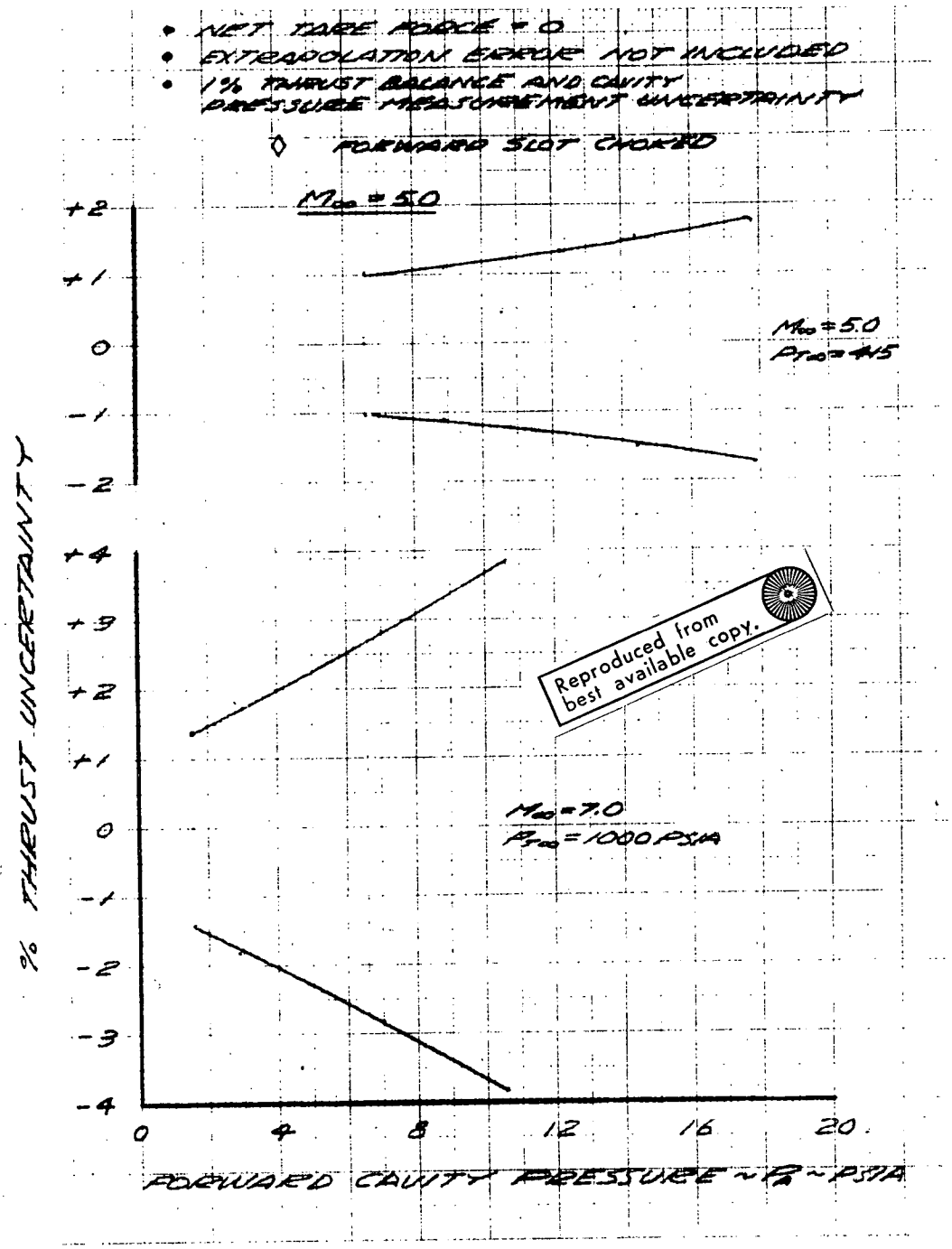

Figure 5-10. Thrust Measurement Uncertainty Due to Purge System Thrust Correction

6. FUTURE ACTION

Effort for the next reporting period will be directed toward:

(a) Assembling the HRE AIM unit and preparing for its shipment to NASA Lewis Research Center, Plumbrook Station.

(b) Finalizing the format for data acquisition and data reduction. Effort will also be expended to interface with the computer facilities of the NASA Lewis Research Center to utilize available computer programs.

(c) Finalizing the test plan for the HRE AIM.

REFERENCES

1. Andersen, W. L., "HRE N_2 Purge System", AiResearch Memo EWLA-0483-1204, December 4, 1970.

2. Sainio, W. C., "Estimated Accuracy of AIM Performance as Determined From Thrust Measurements", AiResearch Memo EWCS-0076-0310, March 10, 1970.

3. Vick, Allen R., "An Investigation to Determine the Discharge and Thrust Characteristics of Auxiliary-Air Outlets for a Free Stream Mach Number of 3.25", NASA TND 1478, October 1962.

4. Engineering Staff, Hypersonic Research Engine Project - Phase II, Aerothermodynamic Integration Model Development Seventh Interim Technical Data Report (U), Data Item 55-4.07, AiResearch Report AP-69-5899, January 16, 1970. CONFIDENTIAL